

Dynamic properties of polyvinylmethylether near the glass transition

R. Casalini^{a)} and C. M. Roland^{b)}

Naval Research Laboratory, Chemistry Division, Code 6120, Washington D.C. 20375-5342

(Received 25 March 2003; accepted 23 May 2003)

Dielectric spectroscopy, encompassing 13 decades of frequency, was used to investigate local segmental relaxation in polyvinylmethylether (PVME). Measurements were obtained over a 110 degree range of temperatures, at pressures up to 725 MPa. At atmospheric pressure, time-temperature superpositioning is valid; however, application of pressure changes the shape of the dielectric spectrum. Similarly, the relaxation times and dc-conductivity have the same temperature dependence at ambient pressure, while a breakdown of the Debye–Stokes–Einstein relation is observed at elevated pressures. The pressure dependence of the relaxation times is weak, corresponding to an activation volume about equal in magnitude to the molar volume of the PVME repeat unit. The pressure coefficient of the glass transition temperature ($T_g = 247.5$ K at ambient pressure) is small, 177 K/GPa. From the ratio of the isochronic and isobaric expansivities, $\alpha = 2.2$, thermal energy is found to have a stronger effect on the relaxation times than does the volume, although the contribution from the latter is significant. A comparison was made of the relaxation properties of PVME to those of the structurally similar polyvinylacetate. Distinct, qualitative differences are noted at both ambient and elevated pressure. © 2003 American Institute of Physics. [DOI: 10.1063/1.1592500]

INTRODUCTION

Among the myriad complex behaviors exhibited by polymers, their local segmental dynamics ranks among the most intriguing and significant. Referred to variously as the glass transition, structural relaxation, dielectric α -relaxation, etc., this process underlies all motions at longer times and length scales. Indeed, it is not uncommon (albeit incorrect^{1,2}) to suppose that all viscoelastic mechanisms, from local segmental relaxation to the terminal chain modes and viscosity, have the same temperature dependence. Clearly, understanding structure-property relationships in polymers, which is essential to their utilization, requires unraveling of the complexities of local segmental relaxation, including the roles played by density and temperature in controlling segmental relaxation and the relationship to the chemical structure. Moreover, the various glass transition phenomena are not unique to long chain molecules, but have been observed, and often first discovered, in supercooled, small-molecule glass formers.^{3–6}

In this work, two aspects of local segmental relaxation in polymers are addressed. The first concerns the origin of the dramatic increase in viscosity and relaxation time as the material is cooled (or compressed) toward the glassy state. Decreasing temperature reduces thermal energy, thus impeding activated transport of chain segments over the potential barriers obstructing passage to new positions and orientations. As embodied in energy landscape models for the glass transition,^{7–9} the details of the potential energy hypersurface govern the dynamic properties, and potentially provide a link to thermodynamic properties.^{10–13}

A decreasing volume is another characteristic of the glass transition and, indeed, compression alone can bring about vitrification. Packing density plausibly influences the congested motion of relaxing segments, and free volume models of the glass transition are well-developed.^{14–16} Since temperature variations change both thermal energy and the volume, it is unsurprising that, when compared on an equal-volume basis, temperature has a stronger effect on the dynamics than pressure. However, at least in principle, both variables contribute. The relative importance of thermal energy and volume is intensely debated,^{17–25} with contrary viewpoints expressed. Temperature has been described as the dominant variable,^{21,22} or at least the more important one,^{17–20} while other experimental evidence suggests that the relative importance of volume and temperature is strongly dependent on the nature of the material, with volume becoming as or even more important than temperature in some cases.^{23–25} Thus, quantifying the relative contribution of thermal energy and volume to the relaxation times is a central issue in studying the glass transition.

The second feature of the glass transition addressed herein is the decoupling often observed between different dynamical processes. The viscosity, relaxation times, diffusion constants, etc. all change drastically as T_g is approached from above, yet their respective temperature dependences can differ substantially. In particular, there is a strong enhancement of diffusion and translational motions relative to reorientations.^{5,26,27} The origin of this phenomenon is uncertain, but it has been ascribed to heterogeneity, either spatially^{26,28} or of the dynamics.²⁹ An understanding of why different processes respond differently to changes in the local structure can yield fundamental insights into structure-property relationships.

In this paper we describe dielectric measurements on

^{a)}Electronic mail: casalini@ccs.nrl.navy.mil

^{b)}Electronic mail: roland@nrl.navy.mil

polyvinylmethylether (PVME) addressing these two aspects of the glass transition. From data obtained both as a function of temperature and of pressure, we determine the volume dependence of the relaxation times, and thereby assess the relative contribution of temperature and volume to the relaxation. We also compare both the temperature and pressure dependence of the conductivity, a transport property, to the corresponding behavior of the dielectric relaxation times.

EXPERIMENT

The PVME, obtained from Scientific Polymer Products and used as received, had a weight average molecular weight 99 000 daltons and a polydispersity=2.1. To remove any absorbed water, the polymer was dried overnight in vacuum at $\sim 60^\circ\text{C}$ prior to measurements, and maintained in a nitrogen atmosphere during the measurements at atmospheric pressure, and in the absence of air during the high pressure measurements.

Dielectric spectra were obtained with an IMASS time domain dielectric analyzer (10^{-4} – 10^4 Hz), a Novocontrol Alpha Analyzer (10^{-2} – 10^6 Hz), and an HP4291A impedance analyzer (10^6 – 10^9 Hz). The latter could only be utilized for ambient pressure experiments, limiting the spectra at elevated pressure to frequencies below 10^6 Hz. For all measurements below 10^6 Hz, the sample was contained between parallel plates. For the high pressure experiments, these plates were inside a Manganin pressure cell (Harwood Engineering), and isolated from the pressurizing fluid by means of a Teflon ring and tape. Pressure was applied using an Enerpac hydraulic pump, in combination with a pressure intensifier (Harwood Engineering), and measured with a Sensotec tensometric transducer (resolution=150 kPa). For the ambient pressure measurements above 10^6 Hz, an HP16453A test fixture was used. Temperature control for all experiments was at least ± 0.1 K. The measured conductivity is due to impurity ions (contaminants); however, replicate testing of different samples gave identical results. Furthermore, the conductivity, as well as the α -relaxation spectra, were insensitive to thermal and pressure histories.

RESULTS

Ambient pressure

Displayed in Fig. 1 are representative dielectric permittivity, ϵ' , and loss, ϵ'' curves as a function of frequency. The dispersion shifts towards lower frequencies with decreasing temperature, concomitant with a small but systematic increase in the dielectric strength, $\Delta\epsilon$. Adjusting for the latter, the peak shape is found to be invariant to temperature (Fig. 2); that is, at constant (ambient) pressure, segmental relaxation in PVME conforms to time-temperature superpositioning. The central portion of the peak can be described using the transform of the Kohlrausch function³⁰

$$\epsilon''(\omega) = \Delta\epsilon \int_0^\infty dt \left[\frac{-d}{dt} \exp-(t/\tau_K)^\beta \right] \sin(\omega t), \quad (1)$$

with a temperature independent $\beta=0.47$. τ_K is the time for the relaxation to decay to e^{-1} of its initial value. The fre-

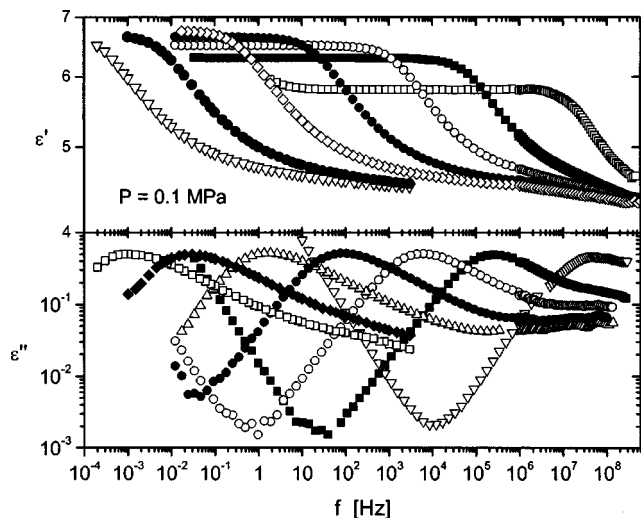


FIG. 1. Double logarithmic plots of the dielectric permittivity and loss measured at ambient pressure and $T = -19$ (\diamond), -9 (\bullet), 6 (\circ), 26 (\blacksquare), and 85 C (\square). The data above 10^6 Hz were obtained with the HP4291 A impedance analyzer.

quency of the maximum in the dielectric loss defines (approximately) the most probable relaxation time, $\tau = 1/(2\pi f_{\max})$; for $\beta=0.47$, $\tau = 1.38 \times \tau_K$. These τ are plotted in Arrhenius form in Fig. 3.

Evident on the low-frequency side of the segmental relaxation dispersion is the dc-conductivity, σ , contribution to the dielectric loss

$$\sigma = 2\pi f \epsilon_0 \epsilon'', \quad (2)$$

where ϵ_0 is the vacuum permittivity. The Stokes–Einstein relation for the diffusion of spheres in a homogenous medium of viscosity η is commonly used to describe ion diffusion, leading to an expected proportionality between σ and η^{-1} . Since the dipolar relaxation time in a homogenous medium is also proportional to viscosity (Debye relation), the

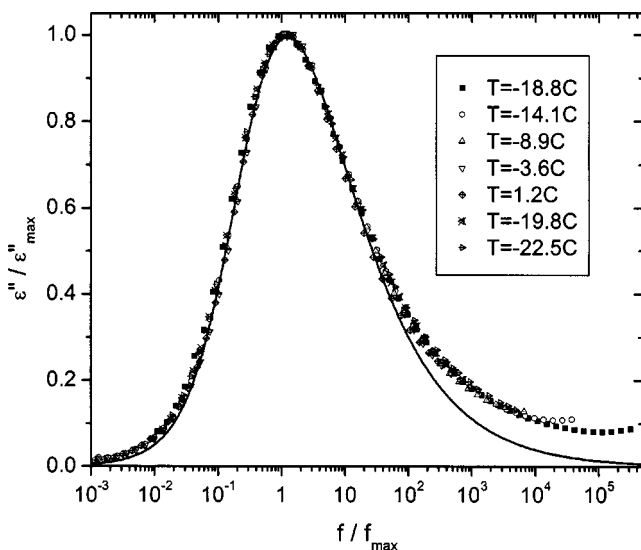


FIG. 2. Superposed dielectric loss spectra for ambient pressure at the indicated temperatures. The solid line is the transform of the Kohlrausch function [Eq. (1)] with $\beta=0.47$.

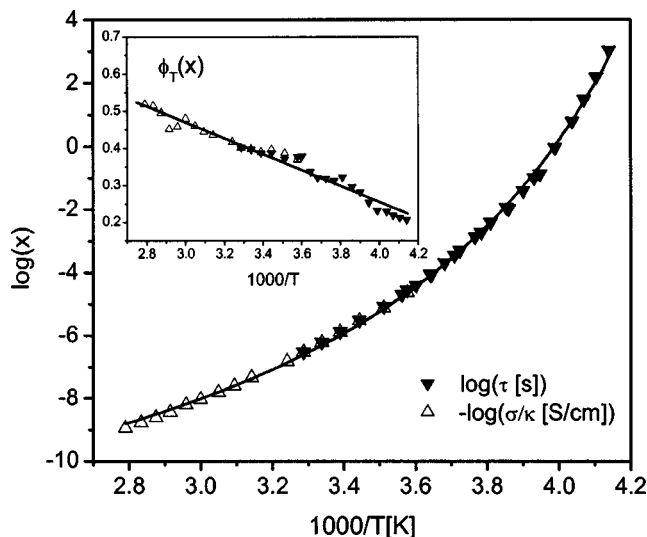


FIG. 3. Relaxation times (filled symbols) and inverse dc-conductivity (hollow symbols) (the latter divided by a constant factor = $10^{20.3}$) as a function of inverse temperature at ambient pressure. The lines through the data represent fits to the Vogel–Fulcher equation. The inset shows the Stickel function Φ for both the conductivity and the relaxation times.

ionic conductivity and the dielectric relaxation times are related by the Debye–Stokes–Einstein (DSE) equation³¹

$$\frac{\sigma \tau T}{c} = \text{const}, \quad (3)$$

in which c is the concentration of charges. Although the rationale for Eq. (3) relies on several approximations, it has intuitive appeal; other derivations³² can also be used to obtain it. Since c is constant, a double logarithmic plot of σT versus relaxation time should have a slope of negative unity.

We show such a plot in Fig. 4 for those temperatures at which both quantities could be obtained from the dielectric measurements without extrapolation. The least squares fit of the slope yields -0.98 ± 0.01 ; thus, at atmospheric pressure the data essentially conform to the DSE equation. Also dis-

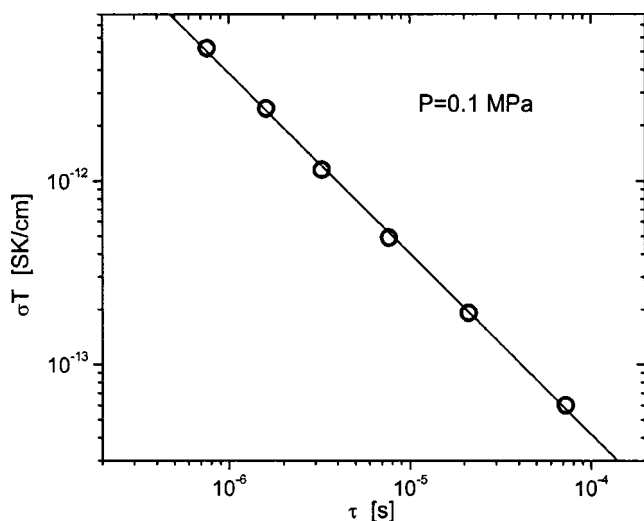


FIG. 4. Relationship between the dc-conductivity and the relaxation time for isobaric ($P=0.1$ MPa) data. The best-fit to the data, indicated by the straight line, has a slope equal to -0.98 ± 0.01 .

played in Fig. 3, are the inverse σ divided by an appropriate factor ($\kappa = 10^{20.3}$ deduced from Fig. 3), such that the two sets of data superpose over their common range of temperatures.

The usual practice is to describe the temperature dependence of τ and σ^{-1} by the Vogel–Fulcher (VF) equation¹⁴

$$x = x_{\infty} \exp\left(\frac{B}{T - T_0}\right), \quad (4)$$

where x is either τ or σ^{-1} , T_0 is the Vogel temperature, B is a constant and x_{∞} is the high-temperature limiting value of x . Deviation from VF behavior can be assessed from plots of the derivative function $\Phi(x)$, the so-called Stickel function³³

$$\Phi(x) = \left\{ \left[\frac{d \log_{10}(x)}{d(1000/T)} \right] \right\}^{-1/2}, \quad (5)$$

which yields a straight line for a VF dependence. In the inset of Fig. 3 is shown the function $\Phi(x)$ calculated for τ and σ^{-1} . It is evident that for all temperatures, the data can be described by a single VF relation. From the simultaneous fit of τ and σ^{-1} to Eq. (4), we obtain $\log_{10}(\tau_{\infty}[\text{s}]) = -13.1 \pm 0.1$, $B = 1590 \pm 70$, $T_0 = 198.3 \pm 1$ K and $\log_{10}(\sigma_{\infty}[\text{S/cm}]) = -7.2 \pm 0.1$ (note that this fitting was done using only three variables, since τ_{∞} and σ_{∞} are related by a constant factor).

A dynamic glass transition can be defined as the temperature at which τ assumes an arbitrary value, e.g., 10 s. Interpolating the data in Fig. 3, we obtain $T_g = 247.5 \pm 0.2$ K at atmospheric pressure. The fragility, $m \equiv d \log_{10}(\tau) / d(T_g/T)|_{T=T_g}$ at ambient pressure is obtained from the slope at T_g , yielding $m = 80$. To compare this result with the literature, we recalculate m for $\tau = 100$ s, yielding $m = 85$, which is larger than the value of 75 previously reported.³⁴ However, the latter was based on an extrapolation of measurements which were limited to $f \geq 1$ Hz on a lower molecular weight PVME.³⁵

Elevated hydrostatic pressure

Dielectric measurements were carried out isothermally, at three different temperatures, as a function of pressure. In Fig. 5, four dielectric loss spectra are shown, for temperatures and pressures such that the maxima in the loss peaks coincide. Unlike the good superpositioning obtained with the ambient pressure spectra (Fig. 2), there is a systematic narrowing on the high-frequency side of the peaks with increasing pressure (and increasing temperature) at constant τ . Since time-temperature superpositioning is observed at atmospheric pressure, Fig. 5 implies a failure of time-pressure superposition, contrary to the results reported from measurements over a more limited pressure range^{36,37} An assessment of time-temperature superpositioning at elevated pressures cannot be made with the available data.

The relaxation times from all measurements at elevated pressure, along with the conductivity data, are displayed in Fig. 6. It is common to parameterize pressure dependences in terms of an activation volume,³⁸ $\Delta V_{\tau}^{\#} = RT(\partial \ln \tau / \partial P)|_T$, or for the conductivity $\Delta V_{\sigma}^{\#} = -RT(\partial \ln \sigma / \partial P)|_T$. At higher pressures, the data deviate from this simple relationship, with an increase of the activation volume as seen in Fig. 6. Such a deviation was not observed in a previous study³⁷ because of the more limited pressure range ($P < 280$ MPa); however,

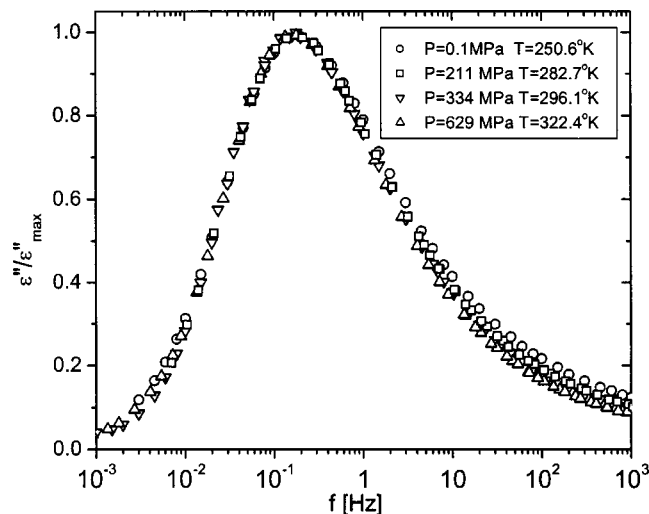


FIG. 5. Superposed dielectric loss spectra as a function of pressure, for various temperatures such that the relaxation times are almost equal (frequencies were shifted by less than 30%).

the $\Delta V_{\tau}^{\#}$ are in agreement where the respective data coincide. More interestingly, the pressure sensitivity is greater for τ than for σ . For example, at the highest temperature, in the limit of zero pressure, $\Delta V_{\tau}^{\#} = 64$ ml/mol for τ versus $\Delta V_{\sigma}^{\#} = 54$ ml/mol. This difference increases inversely with temperature. The magnitude of the activation volume is on the order of the molar volume, $= 54.7$ ml/mol at $T_g = 247.5$ °K and $P = 0.1$ MPa.³⁹

The variation of T_g with pressure is obtained from the temperature at which $\tau = 10$ s at each pressure. These data are plotted in Fig. 7, along with the fit to the empirical Andersson equation⁴⁰

$$T_g = a \left(1 + \frac{b}{c} P \right)^{1/b}, \quad (6)$$

with $a = 248 \pm 0.2$ K, $b = 4.32 \pm 0.08$, and $c = 1.40 \pm 0.02$ GPa. In the limit of zero pressure, $dT_g/dP = 177$

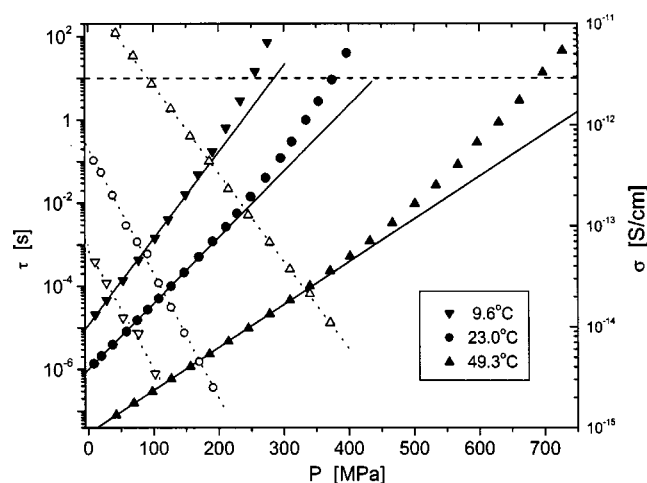


FIG. 6. Relaxation times (filled symbols) and dc-conductivity (hollow symbols) as a function of pressure at the indicated temperatures. The lines through the data represent linear fits to the low pressure measurements, with slopes proportional to respective activation volumes. The horizontal dashed line denotes the value of $\tau = 10$ s at T_g .

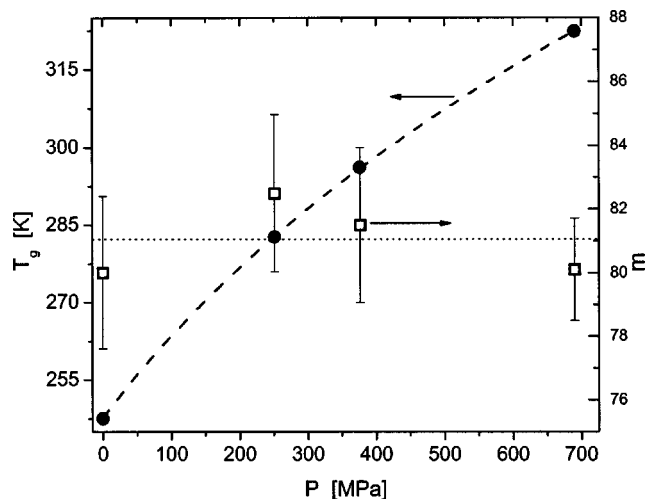


FIG. 7. Pressure dependence of the glass transition temperatures from Fig. 6 (●), and of the fragility (□). The dashed line is the fit to Eq. (6), while the dotted line is an average of the $m(P)$.

± 2 K/GPa. This value is lower than reported previously³⁷ probably because over a more limited range of pressure, T_g appears to be linear with pressure.⁴¹ From the pressure coefficient of the glass transition, we calculate the fragility from the activation volume using⁴²

$$m = \frac{\Delta V^{\#}}{R \ln(10) dT_g/dP}, \quad (7)$$

where both $\Delta V^{\#}$ and dT_g/dP are functions of pressure. These results are included in Fig. 7. Within the experimental uncertainty, the temperature sensitivity of the relaxation times is independent of pressure.

Unlike the results for ambient pressure (Fig. 4), the conductivity and relaxation times measured at elevated pressure are at odds with the DSE relation [Eq. (5)]. This is usually the case for supercooled liquids and polymer melts not far from T_g , even at ambient pressure. Commonly, such behavior is accounted for by an empirical modification of the DSE⁴³

$$\sigma \tau^k = \text{const}, \quad (8)$$

where the adjustable parameter $k \leq 1$. This relation has been applied to data on various glass formers.^{25,43–46} In Fig. 8, we plot double-logarithmically the conductivity as a function of the relaxation times. The elevated pressure data yield different curves for each temperature, with the deviation from the DSE increasing with decreasing temperature. Thus, the DSE fails for the isothermal data (conformance of isobaric results at elevated pressure cannot be judged from the available data).

DISCUSSION

Although pressure exerts a substantial effect on the segmental relaxation times of PVME, it is less sensitive to pressure than most other polymers. The activation volume is roughly comparable to the molar volume, and the pressure coefficient of the glass transition temperature is the lowest

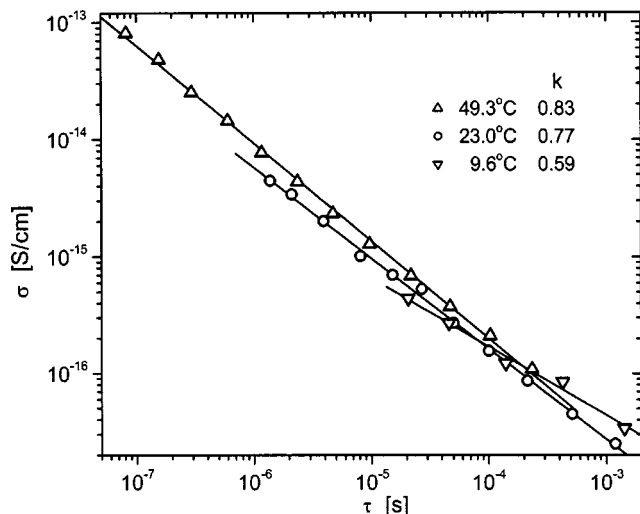


FIG. 8. Relationship between the dc-conductivity and the relaxation time for isothermal data at the indicated temperatures. The lines are fits to Eq. (8), with the fractional Debye–Stokes–Einstein exponents as indicated.

reported to date for any polymer^{25,47–52} (Table I). The value of dT_g/dP is not correlated with either T_g or the sensitivity of the relaxation times to temperature.

To interpret the temperature and pressure dependences of the relaxation times for PVME, the results in Figs. 3 and 6 are expressed as a function of volume. To do this, we take advantage of PVT (pressure–volume–temperature) data for PVME (of the same weight average molecular weight) reported by Ougizawa *et al.*³⁹ The dependence of the specific volume (in ml/g) on temperature (in Celsius) and pressure (in MPa) can be described above using the Tait equation⁵³

$$V(T, P) = (\nu_0 + \nu_1 T + \nu_2 T^2) \times [1 - 0.0894 \ln(1 + P/b_0 \exp(-b_1 T))]. \quad (9)$$

Fitting the data in Ref. 39, we obtain $\nu_0 = 0.9564$ ml/g, $\nu_1 = 5.587 \times 10^{-4}$ ml/g-C, $\nu_2 = 4.256 \times 10^{-7}$ ml/g-C², $b_0 = 236.0$ MPa, and $b_1 = 4.745 \times 10^{-3}$ C⁻¹. We then calculate the specific volume for each temperature and pressure of our measurements, obtaining the results shown in Fig. 9. For a given volume change, there is a substantially larger change in τ along the isobaric pathway than for the isotherms. This

TABLE I. Pressure coefficient of T_g measured dielectrically for various polymers.

	dT_g/dP^a [K/GPa]	Ref.
polymethyltolylsiloxane	340	47
polymethylphenylsiloxane	290	48
polyvinylacetate	250	49
oligomeric epoxy ^b	244	25
1,2-polybutadiene	240	52
polyisobutylene ^c	240	50
oligomeric epoxy ^d	180	51
polyvinylmethylether	177	this work

^a $1 \text{ s} \leq \tau(T_g) \leq 100 \text{ s}$ and $P = 0.1 \text{ MPa}$.

^b diglycidylether of bisphenol-A.

^c from PVT measurements.

^d 4,4'-methylene-bis(N,N-diglycidylaniline).

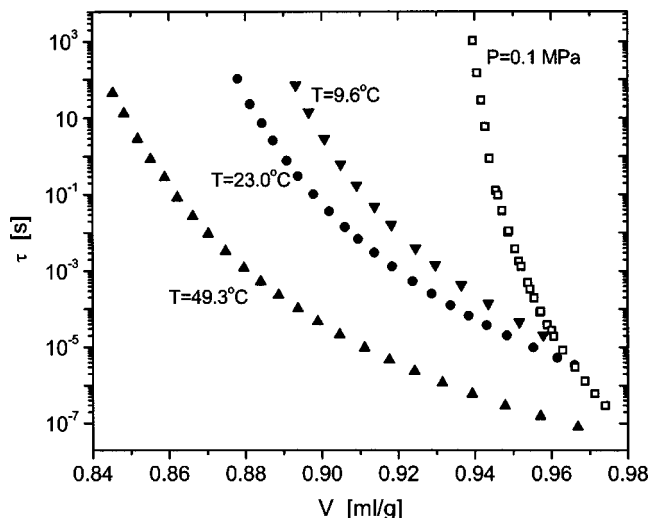


FIG. 9. Isothermal (solid symbols) and isobaric (hollow symbols) relaxation times as a function of specific volume.

is because temperature changes both the thermal energy and the volume, whereas pressure affects only the latter.

To quantify the degree to which these variables govern the relaxation times, we compare the expansivity at constant pressure, $\alpha_p = -V^{-1}(\partial V/\partial T)_p$, to its magnitude at fixed value of the relaxation time, $\alpha_\tau = -V^{-1}(\partial V/\partial T)_\tau$. The ratio of the isochronic and isobaric expansivities, $|\alpha_\tau|/\alpha_p$, will be significantly larger than one if temperature, rather than volume, is the dominant variable controlling the relaxation times.²² From Eq. (9), we obtain $\alpha_p = 5.584 \times 10^{-4} \text{ C}^{-1}$. The specific volume at which $\tau = 10 \text{ s}$ is calculated for each condition, using the data in Figs. 3 and 6, along with Eq. (9). The result, shown in Fig. 10, is $\alpha_\tau = -1.21 \times 10^{-3} \text{ C}^{-1}$. The ratio $|\alpha_\tau|/\alpha_p = 2.2$, is not too far from unity, indicating that although thermal energy changes are more important than volume changes, the contribution of the latter to the relaxation times is still significant. The value of $|\alpha_\tau|/\alpha_p$ for PVME is larger than found for other polymers and molecular

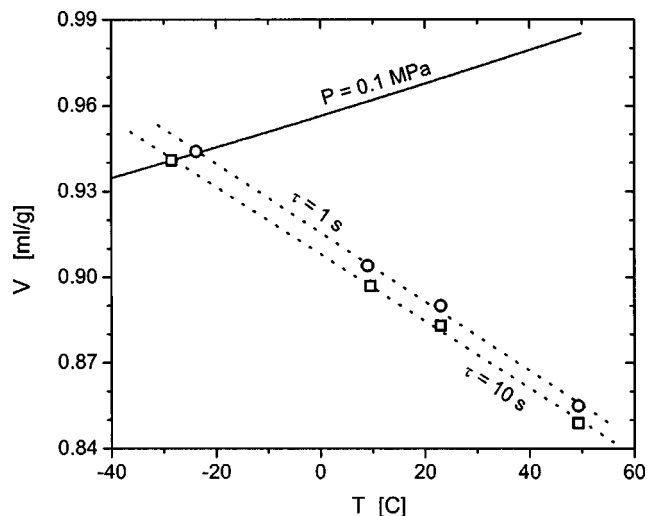


FIG. 10. Temperature dependence of the specific volume at $P = 0.1 \text{ MPa}$ (solid line) and at varying pressures corresponding to a constant $\tau = 1 \text{ s}$ (○) and 10 s (□), respectively.

glass formers, at least in the absence of hydrogen bonding.²³ Also shown in Fig. 10 are results for $\tau=1$ s, which yields $|\alpha_\tau|/\alpha_p=2.1$. Thus, our conclusion regarding the relative significance of temperature and volume is not overly sensitive to the particular condition of T and P at which the assessment is made.

Another quantity which can be used to quantify the relative effect of thermal energy and volume is the ratio of the constant volume activation energy, $E_V(=R[\partial \log(\tau)/\partial(T^{-1})_V])$, to the activation energy at constant pressure, $E_P(=R[\partial \log(\tau)/\partial(T^{-1})_P])$. This latter quantity (which is more correctly referred to as the activation enthalpy) can be directly estimated from dielectric relaxation data, if the measurements extend over a sufficient frequency range, or alternatively by using the relation¹⁹

$$\frac{E_V}{E_P} = 1 - \gamma \left(\frac{\partial T}{\partial P} \right)_\tau, \quad (10)$$

where $\gamma[(\partial P/\partial T)_V]$ is the thermal pressure coefficient calculated from the PVT data. For $V=0.9424$ mL/g (corresponding to T_g at ambient pressure), we obtain $\gamma=1.70$ MPa/K. Using the pressure dependence of T_g , we then calculate $E_V/E_P=0.7$. This value is larger than $E_V/E_P=0.67$ found for PVAc,⁴⁹ but smaller than the values of 0.73 reported for polypropylene oxide¹⁹ (PPO) and 0.71–0.78 for polymethyl acrylate¹⁸ (PMA).⁵⁴ The ratio E_V/E_P would equal 1 or 0 if the temperature or volume dominates, respectively.

The ratio E_V/E_P is related to the ratio of the thermal expansivities as

$$\frac{E_V}{E_P} = \frac{1}{1 - \alpha_p/\alpha_\tau}. \quad (11)$$

This relation is derived in the Appendix. In Fig. 11, Eq. (11) is plotted, along with values for PVME and other glass formers (taken from the literature). By either measure, thermal energy is seen to be more important than volume in governing the temperature dependence of the relaxation times of PVME. The differing influences of temperature and volume are manifested in other properties. The relaxation times are more sensitive to pressure than is the conductivity, and the relationship between these two quantities under isobaric conditions (Fig. 4) is distinct from their isothermal behavior (Fig. 8). In fact, the fractional DSE exponent at elevated pressure is different for each temperature. This behavior differs markedly from results reported for other glass formers, for example, the epoxy resin, poly(phenyl glycidyl ether)-co-formaldehyde.⁵⁵ For PVME, the isobaric data conform to the DSE, while the isothermal results show the more usual deviation (translation and diffusion enhanced relative to reorientation^{26,27}).

Decoupling of these motions has been ascribed to spatially heterogeneous dynamics, considering that rotational and translational mobilities average in different ways over the sample.^{26–29} The progressive decoupling shown in Fig. 8 would, therefore, indicate an increase of the heterogeneity with pressure in proximity of T_g . However, as pointed out previously by other authors,^{29,56} an explanation based on spa-

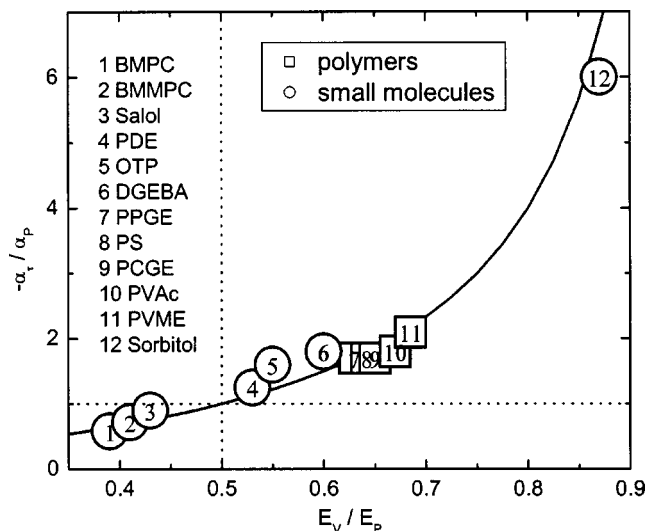


FIG. 11. Ratio of thermal expansivities vs ratio of apparent activation energies for several glass formers: 1,1'-bis(p-methoxyphenyl)cyclohexane (BMPC) (Ref. 24), 1,1'-di(4-methoxy-5-methylphenyl)cyclohexane (BMMPC) (Ref. 24), salol (Ref. 68), phenylphthalein-dimethylether (PDE) (Ref. 23), o-terphenyl (OTP) (Refs. 69 and 70), diglycidylether of bisphenol A (DGEBA) (Ref. 25), poly(phenyl glycidyl ether)-co-formaldehyde (PPGE) (Ref. 23), polystyrene (PS) (Ref. 71), poly[(o-cresyl glycidyl ether)-co-formaldehyde] (PCGE) (Ref. 72), polyvinylacetate (PVAc) (Ref. 49), PVME and d-sorbitol (Ref. 73). Intersection of the dotted lines denotes an equal contribution from volume and temperature. The solid line is Eq. (11).

tial heterogeneity cannot account in general for the enhancement of dielectric relaxation times compared with rotational diffusion, since both are local motions probing the same environment.

The failure of time–temperature–pressure superpositioning may reflect an intermolecular cooperativity that varies with pressure,⁵⁷ as indicated by the changing shape of the relaxation peak (Fig. 5). However, the latter could be influenced by a different response to pressure of the primary segmental relaxation and an unresolved higher frequency secondary process.^{58–60} Unambiguous interpretation of this phenomenon would require measurements over a broader range of frequencies at even higher pressures.

Finally, it is of interest to compare the dynamic properties of PVME to those of the structurally similar polyvinylacetate (PVAc).^{49,61,62} The latter differs only by the replacement of the pendant methyl group with a methyl-substituted carbonyl. At atmospheric pressure, the properties of the two polymers differ significantly (Table II). The glass transition temperature (defined as $\tau=10$ s) for PVAc is 56 degrees higher than PVME, although the latter is substantially more fragile. Despite the difference in m , the respective peak breadths at T_g are essentially equal. This absence of a correlation between fragility and peak breadth is unusual,³⁴ and may be related to the fact that the dipole moment in PVAc is further removed from the backbone than for PVME. It is also noteworthy that at atmospheric pressure, while the breadth of the segmental relaxation peak for PVME is invariant to temperature (Fig. 2), that of PVAc broadens significantly with cooling toward T_g .^{61,62} A comparison of the properties of these two polymers by other spectroscopies, such as mechanical measurements, would be illuminating.

TABLE II. Comparison of local segmental relaxation properties.

	PVME	PVAc (Refs. 49, 61, and 62)
T_g^a	247.6	303.6
β^b	0.47	0.48
$d\beta/dT^b$	0	$\approx 0.003 \text{ K}^{-1}$
m^a	81	76
dm/dP	0	0
$V^\# / V_m^c$	≈ 1.1	≈ 2
$ \alpha_\tau / \alpha_P^a$	2.2	1.8

^a $\tau(T_g) = 10 \text{ s}$ and $P = 0.1 \text{ MPa}$.

^b $T > T_g$.

^c $P \approx 0.1 \text{ MPa}$.

Fundamental differences in the behavior of these two polymers are also evident at elevated pressure (Table II). Near T_g , the activation volume of PVAc is more than twice the molar volume, whereas for PVME these two quantities differ by less than 20%. Related to this difference, the pressure coefficient of T_g is markedly higher for PVAc (Table I). However, the temperature dependence of the relaxation times for both polymers varies insignificantly with pressure. Whether the differing effects of pressure for PVAc is related to the fact that temperature and volume have a more nearly equal role in governing the magnitude of its relaxation times, in comparison to PVME (Table II), is unclear.

CONCLUSIONS

Pressure and temperature have a qualitatively different effect on the dynamics of PVME. This is seen in the variation with pressure of the shape of the dispersion in the dielectric loss and the Debye–Stokes–Einstein fractional exponent. These results differ from behavior observed for other polymers^{48,49,55,63} and molecular glass formers^{25,46,64–67}. The pressure coefficient of T_g for PVME is also the smallest reported to date for any polymer. From analysis of the isochronic and isobaric thermal expansivities, the degree to which the magnitude of the relaxation times is governed by temperature and pressure was quantified. We find that both thermal energy and volume exert a significant effect, although the former is more dominant. The segmental relaxation properties of PVME at both ambient and elevated pressure are conspicuously different from those of PVAc, despite the similarity in chemical structure of the two polymers

ACKNOWLEDGMENTS

This work was supported by the Office of Naval Research. The authors thank K. L. Ngai for stimulating discussions and the referee for suggesting the use of Eq. (11).

APPENDIX: RELATIONSHIP BETWEEN ACTIVATION ENERGY RATIO AND THERMAL EXPANSION COEFFICIENT RATIO

Equation (11) can be derived by first expressing the temperature derivative of the volume at constant τ as

$$\left. \frac{\partial V}{\partial T} \right|_{\tau} = \left. \frac{\partial V}{\partial T} \right|_P + \left. \frac{\partial V}{\partial P} \right|_T \left. \frac{\partial P}{\partial T} \right|_{\tau}. \quad (\text{A1})$$

Dividing both sides by the temperature derivative of the volume at constant pressure gives

$$\left. \frac{\partial V}{\partial T} \right|_{\tau} / \left. \frac{\partial V}{\partial T} \right|_P = \frac{\alpha_{\tau}}{\alpha_P} = 1 + \left(\left. \frac{\partial V}{\partial P} \right|_T / \left. \frac{\partial V}{\partial T} \right|_P \right) \left. \frac{\partial P}{\partial T} \right|_{\tau}. \quad (\text{A2})$$

From the rule of the implicit partial derivative, the value in brackets is just the negative pressure derivative of temperature at constant volume; thus,

$$\frac{\alpha_{\tau}}{\alpha_P} = 1 - \left. \frac{\partial T}{\partial P} \right|_V \left. \frac{\partial P}{\partial T} \right|_{\tau}. \quad (\text{A3})$$

Comparing Eq. (A3) with Eq. (10) yields Eq. (11), directly relating the two measures of volume and temperature effects.

- ¹D. J. Plazek, I. C. Chay, K. L. Ngai, and C. M. Roland, *Macromolecules* **28**, 6432 (1995).
- ²C. M. Roland, K. L. Ngai, P. G. Santangelo, X. H. Qiu, M. D. Ediger, and D. J. Plazek, *Macromolecules* **34**, 6159 (2001).
- ³C. Hansen, F. Stickel, T. Berger, R. Richert, and E. W. Fischer, *J. Chem. Phys.* **107**, 1086 (1997).
- ⁴P. Lunkenheimer, *Dielectric Spectroscopy of Glassy Dynamics, Habilitationsschrift, Univ. Augsburg* (Shaker, Aachen, 1999).
- ⁵M. D. Ediger, *Annu. Rev. Phys. Chem.* **51**, 99 (2000).
- ⁶C. A. Angell, K. L. Ngai, G. B. McKenna, P. F. McMillan, and S. W. Martin, *J. Appl. Phys.* **88**, 3113 (2000).
- ⁷M. Goldstein, *J. Chem. Phys.* **51**, 3728 (1969).
- ⁸C. A. Angell, *Nature (London)* **393**, 521 (1998).
- ⁹S. Sastry, P. G. Debenedetti, and F. H. Stillinger, *Nature (London)* **393**, 554 (1998).
- ¹⁰R. Richert and C. A. Angell, *J. Chem. Phys.* **108**, 9016 (1998); L. M. Martinez and C. A. Angell, *Nature (London)* **410**, 663 (2001).
- ¹¹O. Yamamuro, I. Tsukushi, A. Lindqvist, S. Takahara, M. Ishikawa, and T. Matsuo, *J. Phys. Chem. B* **102**, 1605 (1998).
- ¹²C. M. Roland, P. G. Santangelo, and K. L. Ngai, *J. Chem. Phys.* **111**, 5593 (1999).
- ¹³C. G. Robertson, P. G. Santangelo, and C. M. Roland, *J. Non-Cryst. Solids* **275**, 153 (2000).
- ¹⁴J. D. Ferry, *Viscoelastic Properties of Polymers*, 3rd ed. (Wiley, New York, 1980).
- ¹⁵M. H. Cohen and G. S. Grest, *Phys. Rev. B* **20**, 1077 (1979).
- ¹⁶J. T. Bendler, J. J. Fontanella, and M. F. Shlesinger, *Phys. Rev. Lett.* **87**, 195503 (2001).
- ¹⁷G. Williams, in *Dielectric Spectroscopy of Polymeric Materials*, edited by J. P. Runt and J. J. Fitzgerald (ACS, Washington D.C., 1997).
- ¹⁸G. Williams, *Trans. Faraday Soc.* **60**, 1556 (1964).
- ¹⁹G. Williams, *Trans. Faraday Soc.* **61**, 1564 (1965).
- ²⁰G. Williams, *Trans. Faraday Soc.* **60**, 1548 (1964).
- ²¹C. Alba-Simionesco, D. Kivelson, and G. Tarjus, *J. Chem. Phys.* **116**, 5033 (2002).
- ²²M. L. Ferrer, C. Lawrence, B. G. Demirjian, D. Kivelson, C. Alba-Simionesco, and G. Tarjus, *J. Chem. Phys.* **109**, 8010 (1998).
- ²³M. Paluch, R. Casalini, and C. M. Roland, *Phys. Rev. B* **66**, 092202 (2002).
- ²⁴M. Paluch, R. Casalini, C. M. Roland, G. Meier, and A. Patkowski, *J. Chem. Phys.* **118**, 4578 (2003).
- ²⁵M. Paluch, C. M. Roland, J. Gapinski, and A. Patkowski, *J. Chem. Phys.* **118**, 3177 (2003).
- ²⁶D. Ehlich and H. Sillescu, *Macromolecules* **23**, 1600 (1990); I. Chang and H. Sillescu, *J. Phys. Chem. B* **101**, 8794 (1997).
- ²⁷T. Inoue, M. T. Cicerone, and M. D. Ediger, *Macromolecules* **28**, 3425 (1995); M. T. Cicerone, F. R. Blackburn, and M. D. Ediger, *ibid.* **28**, 8224 (1995).
- ²⁸M. D. Ediger, *J. Non-Cryst. Solids* **235–237**, 10 (1998).
- ²⁹K. L. Ngai, *J. Phys. Chem. B* **103**, 10684 (1999).
- ³⁰R. Kohrausch, *Pogg. Ann. Phys.* **12**(3), 393 (1847); G. Williams and D. C. Watts, *Trans. Faraday Soc.* **66**, 80 (1970).
- ³¹F. Stickel, E. W. Fisher, and R. Richert, *J. Chem. Phys.* **104**, 2043 (1996).
- ³²P. G. De Gennes, *C. R. Physique* **3**, 1263 (2002).
- ³³F. Stickel, R. Richert, and E. W. Fisher, *J. Chem. Phys.* **102**, 6251 (1995).
- ³⁴R. Böhmer, K. L. Ngai, C. A. Angell, and D. J. Plazek, *J. Chem. Phys.* **99**, 4201 (1993).

- ³⁵ A. Zetsche, F. Kremer, J. Wieland, and H. Schulze, *Polymer* **31**, 183 (1990).
- ³⁶ A. Alegría, D. Gómez, and J. Colmenero, *Macromolecules* **35**, 2030 (2002).
- ³⁷ G. Floudas, in *Broadband Dielectric Spectroscopy*, edited by F. Kremer and A. Schönhal (Springer, Berlin, 2003).
- ³⁸ S. Glasstone, K. Laidler, and H. Eyring, *Theory of Rate Processes* (McGraw-Hill, New York, 1941).
- ³⁹ T. Ougizawa, G. T. Dee, and D. J. Walsh, *Macromolecules* **24**, 3834 (1991).
- ⁴⁰ S. P. Andersson and O. Andersson, *Macromolecules* **31**, 2999 (1998).
- ⁴¹ A more careful comparison with the results in Ref. 37 is not possible because the original data are unpublished.
- ⁴² M. Paluch, J. Gapinski, A. Patkowski, and E. W. Fischer, *J. Chem. Phys.* **114**, 8048 (2001).
- ⁴³ H. Sasabe and S. Saito, *Polymer* **3**, 624 (1972).
- ⁴⁴ T. Koike, *Adv. Polym. Sci.* **148**, 139 (1999).
- ⁴⁵ S. Corezzi, S. Capaccioli, G. Gallone, M. Lucchesi, and P. A. Rolla, *J. Phys.: Condens. Matter* **9**, 6199 (1997).
- ⁴⁶ S. Hensel-Bielowka, T. Psurek, J. Ziolo, and M. Paluch, *Phys. Rev. E* **63**, 062301 (2001).
- ⁴⁷ S. Pawlus, C. M. Roland, S. J. Rzoska, J. Ziolo, and M. Paluch, *Rubber Chem. Technol.* (to be published).
- ⁴⁸ M. Paluch, C. M. Roland, and S. Pawlus, *J. Chem. Phys.* **116**, 10932 (2002).
- ⁴⁹ C. M. Roland and R. Casalini, *Macromolecules* **36**, 1361 (2003).
- ⁵⁰ J. M. O'Reilly, *J. Polym. Sci.* **57**, 429 (1962).
- ⁵¹ R. Casalini, M. Paluch, T. Psurek, and C. M. Roland (to be published).
- ⁵² C. M. Roland, R. Casalini, P. Santangelo, M. Sekula, J. Ziolo, and M. Paluch, *Macromolecules* **36**, 4954 (2003).
- ⁵³ P. G. Tait, *Physics and Chemistry of the Voyage of H. M. S. Challenger* (HMSO, London, 1888), Vol. 2, Part 4.
- ⁵⁴ For PPO and PMA, $(\partial T/\partial P)_\tau$ was calculated at higher temperatures ($\tau < 1$) due to experimental limitations, and thus is not comparable to the other results.
- ⁵⁵ M. Paluch, T. Psurek, and C. M. Roland, *J. Phys.: Condens. Matter* **14**, 9489 (2002).
- ⁵⁶ I. Chang and H. Sillescu, *J. Phys. Chem.* **101**, 8794 (1997).
- ⁵⁷ C. M. Roland and K. L. Ngai, *Macromolecules* **24**, 5315 (1991); **25**, 1844 (1992); **25**, 7031 (1992); K. L. Ngai and C. M. Roland, *ibid.* **26**, 6824 (1993).
- ⁵⁸ G. Williams, *Trans. Faraday Soc.* **62**, 1329 (1966).
- ⁵⁹ G. Williams and D. C. Watts, *Trans. Faraday Soc.* **67**, 1971 (1971).
- ⁶⁰ G. Williams and D. C. Watts, *Trans. Faraday Soc.* **67**, 2973 (1971).
- ⁶¹ F. Stickel, PhD thesis, Johannes Gutenberg University, Mainz, Germany (Shaker, Achen, 1995).
- ⁶² K. L. Ngai and C. M. Roland, *Polymer* **42**, 567 (2002).
- ⁶³ M. Paluch, S. Pawlus, and C. M. Roland, *Macromolecules* **35**, 7338 (2002).
- ⁶⁴ T. Psurek, S. Hensel-Bielowka, J. Ziolo, and M. Paluch, *J. Chem. Phys.* **116**, 9882 (2002).
- ⁶⁵ C. M. Roland, R. Casalini, and M. Paluch, *Chem. Phys. Lett.* **367**, 259 (2002).
- ⁶⁶ M. Paluch, K. L. Ngai, and S. Hensel-Bielowka, *J. Chem. Phys.* **114**, 10872 (2001).
- ⁶⁷ M. Paluch, M. Sekula, S. Pawlus, S. J. Rzoska, C. M. Roland, and J. Ziolo, *Phys. Rev. Lett.* **90**, 175702 (2003).
- ⁶⁸ R. Casalini, M. Paluch, and C. M. Roland, *J. Phys. Chem. A* **107**, 2369 (2003).
- ⁶⁹ M. Naoki, H. Endou, and K. Matsumoto, *J. Phys. Chem.* **91**, 4169 (1987).
- ⁷⁰ C. Dreyfus, A. Aouadi, J. Gapinski, M. Matos-Lopez, W. Steffen, A. Patkowski, and R. M. Pick (unpublished).
- ⁷¹ C. M. Roland and R. Casalini, *J. Chem. Phys.* **119**, 1838 (2003).
- ⁷² C. M. Roland, M. Paluch, T. Pakula, and R. Casalini, *Phil. Mag. B.* (to be published).
- ⁷³ S. Hensel-Bielowka, M. Paluch, J. Ziolo, and C. M. Roland, *J. Phys. Chem. B* **106**, 12459 (2003).